Time-like proton form factor measurement with $\bar{\mathrm{P}}$ANDA

M. Sudol[1)] (for $\bar{\mathrm{P}}$ANDA collaboration)

(Institut de Physique Nucléaire, CNRS/IN2P3, Université Paris Sud, Orsay, France)

Abstract The electromagnetic probe is an excellent tool to investigate the structure of the nucleon. The nearly 4π detector $\bar{\mathrm{P}}$ANDA, will allow to make a precise determination of the electromagnetic form factors of the proton in the time-like region with unprecedented precision. In the one-photon exchange approximation, the center of mass unpolarized differential cross section of the reaction $\bar{\mathrm{p}}\mathrm{p} \to \mathrm{e}^+\mathrm{e}^-$ is a linear combination of the squared moduli of the electric G_{E} and magnetic G_{M} proton form factors. The precise measurement of the angular distribution over almost full angular range then directly gives these quantities. At present only two experiments have provided the ratio $R = |G_{\mathrm{E}}|/|G_{\mathrm{M}}|$ but with large statistical uncertainties. It is shown that with strict PID cuts and a kinematic fit, the dominant background, $\bar{\mathrm{p}}\mathrm{p} \to \pi^+\pi^-$, can be supressed to much less than 1 % of the signal, without affecting the extraction of the ratio R. $\bar{\mathrm{P}}$ANDA will therefore offer a unique opportunity to measure the ratio with a precision ranging from <1% at low q^2 up to 30 % for $q^2 = 14$ (GeV/c)^2 .

Key words electromagnetic form factors, nuclear structure, FAIR, PANDA

PACS 25.43.+t, 13.40.Gp

1 Introduction

Elastic electromagnetic processes represent an important source of information about the hadron structure. Electromagnetic form factors of a hadron are the most direct link to the structure of the hadron in terms of its constituents.

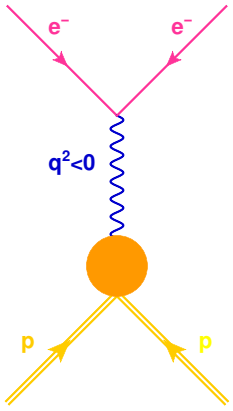

Fig. 1. The Feynman diagram of $\mathrm{ep} \to \mathrm{e}'\mathrm{p}'$ elastic scattering.

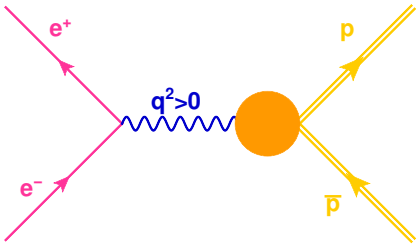

Fig. 2. The Feynman diagram of $\bar{\mathrm{p}}\mathrm{p} \to \mathrm{e}^+\mathrm{e}^-$ annihilation.

Form factors are analytic functions of the four-momentum transfer squared (q^2). These FFs can be measured in two different types of reactions (Figs. 1, 2) corresponding to different kinematical regions. In the space-like region, where q^2 is negative, the physical process is the elastic scattering of an electron on a composite particle. In the time-like region, where q^2 is positive the physical process is the annihilation of a lepton and an anti-lepton followed by the production of a hadron and its corresponding anti-hadron, or the inverse process. In the space-like region the form factors are real, while they are complex functions in the time-like region.

Received 7 August 2009

1) E-mail: sudol@ipno.in2p3.fr

As a spin one half particle, the proton is described by two form factors, the Pauli form factor (F_1) and Dirac form factor F_2 or equivalently electric and magnetic Sachs form factors G_E and G_M.

The latter are defined as follows:

$$G_\mathrm{E} = F_1 + \tau F_2,$$
$$G_\mathrm{M} = F_1 + F_2,$$
$$\tau = \frac{q^2}{4M^2}.$$

Their values at zero momentum transfer are directly related to the charge and magnetization of the hadron. According to the Phragmen-Lindeloef theorem [1], the space-like form factors and the time-like form factors are the same as $q^2 \to \infty$.

$$\lim_{q^2 \to -\infty} F^{SL}(q^2) = \lim_{q^2 \to +\infty} F^{TL}(q^2). \qquad (1)$$

Thus for very large q^2, the time-like form factors become real functions.

Already in 1962 Zichichi[2] proposed to measure the proton form factors by measuring differential cross sections. In the one-photon exchange approximation the differential cross section can be expressed in the following way:

$$\frac{\mathrm{d}\sigma}{\mathrm{d}\cos\theta} = \frac{\pi\alpha^2}{8M^2\sqrt{\tau(\tau-1)}} \times \left[|G_\mathrm{M}^2|(1+\cos^2\theta) + \frac{|G_\mathrm{E}|^2}{\tau}\sin^2\theta \right], \qquad (2)$$

where, θ is the angle between the electron and the proton in the center-of-mass system (CM), α the fine structure constant and M the proton mass. At large momentum transfer separation between G_E and G_M becomes difficult, the relative sensitivity to the electric form factor decreases with incident energy as q^2.

2 The $\bar{\mathrm{P}}$ANDA experiment

The $\bar{\mathrm{P}}$ANDA experiment[3] has a rich experimental program whose ultimate aim is to improve our knowledge of the strong interaction and of the hadron structure. The experimental setup is being designed to fully exploit the extraordinary physics potential arising from the availability of high-intensity, cooled antiproton beams. Significant progress beyond the present understanding of the field is expected thanks to improvements in statistics and precision of the future data. In order to address the different physics topics, it is designed to fulfill many highly demanding requirements: almost full solid angle coverage, momentum resolution on charged particles at a few % level (for 1 GeV/c), capability of detecting with high efficiency both charged and neutral particles in a large momentum range, high rate capabilities and good primary and secondary vertex resolution. Detailed description of the $\bar{\mathrm{P}}$ANDA detector can be found in[3].

The $\bar{\mathrm{P}}$ANDA detector will be installed at the High Energy Storage Ring (HESR[4]) at the future Facility for Antiproton and Ion Research (FAIR[5]). An important feature of the HESR is the availability of two modes: a high resolution (HR) one and a high luminosity (HL) one (see Table 1).

Table 1. Operation modes of the HESR.

mode	HR	HL
p range/(GeV/c)	1.5—9	1.5—15
$\frac{\sigma_p}{p}$	4×10^{-5}	10^{-4}
$L/(\mathrm{cm}^{-2}\cdot\mathrm{s}^{-1})$	2×10^{31}	2×10^{32}

To achieve an almost 4π acceptance and a good momentum resolution over a large range $\bar{\mathrm{P}}$ANDA detector is split into two parts: a Target Spectrometer (TS) placed inside a solenoid magnet for high p_T tracks and a Forward Spectrometer (FS) with dipole magnet for the forward reaction products. The solenoid magnet is super-conducting and has a field of 2 T, the dipole one has a field integral of 2 Tm.

The main components of the target spectrometer will be a microvertex silicon detector, a central tracker (based on a set of Straw tubes or on a TPC), a time-of-flight telescope, a DIRC (Cherenkov detector), an electromagnetic calorimeter equipped with Lead tungstate crystals and a set of muon counters interleaved with iron plates and multiwire drift chambers for tracking at intermediate angles. The forward spectrometer will consist of tracking detectors (straw tubes or multiwire chambers) before, inside and behind the magnet, of a gas Cerenkov, of a time-of-flight detector system and of a Shashlyk calorimeter for hadron/electron identification.

Good particle identification (PID) for charged hadrons and leptons plays an essential role for $\bar{\mathrm{P}}$ANDA and must be guaranteed over a large momentum range from 200 MeV/c up to approximately 10 GeV/c. Several subdetectors provide useful PID information and momenta. While trackers provide energy loss measurements, the DIRC detector is the most suitable device for the identification of particles with momenta above the Cherenkov threshold. Time of flight detectors will also help separating the different particle species. The electromagnetic calorimeter is the most powerful detector for an efficient and clean electron identification. The Muon detector is designed for the separation of muons from the other

particle species. The best PID performance however can be obtained by taking into consideration all available information of all subdetectors. Likelihood for individual sub-detectors have been calculated and parametrized as a function of momentum and angles. When combined altogether, a global likelihood can be obtained on which thresholds can put to do particle identification.

A schematic view of the $\bar{\mathrm{P}}$ANDA detector is shown in Fig. 3.

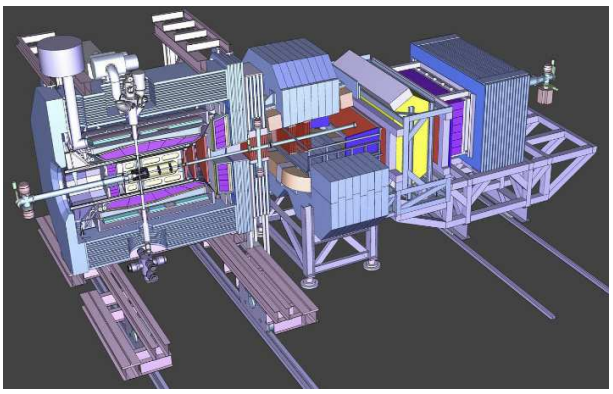

Fig. 3. Layout of the $\bar{\mathrm{P}}$ANDA detector.

3 Electromagnetic form factors with $\bar{\mathrm{P}}$ANDA

3.1 Background channels study

The $\bar{\mathrm{P}}$ANDA experiment will offer a unique opportunity to determine individually the moduli of the two proton time-like form factors. There are two reasons that limit the precision with which the two form factors can be extracted. The first one is the presence of a huge hadronic background, dominated by the reaction $\bar{\mathrm{p}}\mathrm{p}\to\pi^+\pi^-$, about 10^6 higher on average. This implies that a very careful study of the rejection capabilities is necessary. The second one has to deal with the sensitivity of the angular distributions to the ratio $R=|G_{\mathrm{E}}|/|G_{\mathrm{M}}|$. Whereas the cross section decreases steeply with q^2, thus limiting the overall statistics, the $1/\tau$ factor weighting the electric form factor reduces drastically the sensitivity to $|G_{\mathrm{E}}|$ as q^2 increases. Simulation were made to quantify the precision for different q values.

Figure 4[7] shows the ratio of the differential cross section for the reaction $\bar{\mathrm{p}}\mathrm{p}\to\pi^+\pi^-$ with the one for the signal as a function of the cosθ for $q^2=8.21$ (GeV/c)^2. One can clearly see that the cross section for the reaction background channel is by 6 orders of magnitude higher. In this case a rejection factor of at least 10^8 is necessary if one wants to keep the pollution of the signal below 1%. For this reason, in the first step we have simulated the background processes for $\pi^+\pi^-$ with very high statistics for 3 q^2 values.

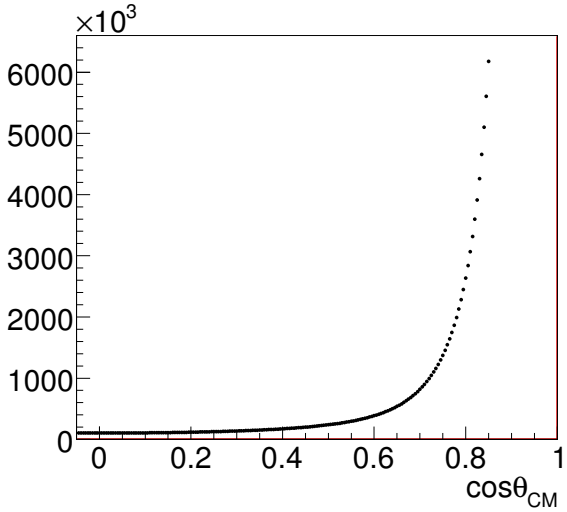

Fig. 4. Ratio of the differencial cross-section for the reaction $\bar{\mathrm{p}}\mathrm{p}\to\pi^+\pi^-$ to $\bar{\mathrm{p}}\mathrm{p}\to\mathrm{e}^+\mathrm{e}^-$ for $q^2=8.21$ (GeV/c)^2.

Using very strict PID cuts (combined PID likelihood equal or larger than 99.8% for each pair candidate) allowed us to reach a rejection factor of the order of few 10^7. In addition to PID, the Confidence Level (CL) cut resulting from the kinematic refit was used. It gives an independent rejection factor of the order of 100, only slightly energy-dependant. Combining the PID cut to the CL on the kinematic fit, a global rejection factor of at least 10^9 can be reached. The corresponding level of contamination of the electron signal is then below 0.3% in the considered angular range at any energy. Within these conditions, the contamination of the e+e signal by $\pi^+\pi^-$ will be well below 1% and will therefore not affect the precision for extracting the magnetic and the electric proton form factors.

The $\bar{\mathrm{p}}\mathrm{p}\to\pi^0\pi^0$ is also a source of possible background, when each of the two π^0's either undergoes a Dalitz decay or two photons, where one or both photons can convert in the detector material present in front of the calorimeter. In the simulations we have considered the following reactions involving π^0:

$$\bar{\mathrm{p}}\mathrm{p}\to\pi^0\pi^0\to\mathrm{e}^+\mathrm{e}^-\gamma\quad \mathrm{e}^+\mathrm{e}^-\gamma\ (\gamma\to\mathrm{e}^+\mathrm{e}^-),$$
$$\bar{\mathrm{p}}\mathrm{p}\to\pi^0\pi^0\to\mathrm{e}^+\mathrm{e}^-\gamma\quad \gamma\gamma\ (\gamma\to\mathrm{e}^+\mathrm{e}^-),$$
$$\bar{\mathrm{p}}\mathrm{p}\to\pi^0\pi^0\to\gamma\gamma\quad \gamma\gamma\ (\gamma\to\mathrm{e}^+\mathrm{e}^-).$$

The first one scales as the π^0 Dalitz decay branching ratio $\Gamma_{\gamma\mathrm{e}^-\mathrm{e}^+}$ squared. The second one scales as

$\Gamma_{\gamma e^- e^+}$ times the conversion probability in the detector material. The third one scales as the conversion probability squared. In all cases the final state is a 6-body one ($2e^-$, $2e^+$, 2γ). From the first reaction, one can deduce that kinematical constraints and $\bar{\mathrm{P}}$ANDA hermeticity provide a rejection factor of at least 10^4 for $\cos\theta = 0$. This factor applies as well to the case with 2 γ conversion. As a result, we can say that the $\pi^0\pi^0$ channel can be rejected by a factor of 10^8 at $\cos\theta = 0$ and by 10^{12} at $\cos\theta = 1$. This high rejection power corresponds to a pollution of the signal by the $\bar{p}p \to \pi^0\pi^0$ events below 1%.

3.2 Signal channel study

The simulation of the signal reaction $\bar{p}p \to e^+e^-$ have been performed at several q^2 values in order to explore the full kinematical range of the reaction from $q^2 = 5.4$ (GeV/c)^2 up to $q^2 = 22$ (GeV/c)^2.

The cross section of the reactions have been taken from data and extrapolated to high q^2 values. Three hypotheses for G_{E} have been taken into account: $|G_{\mathrm{E}}| = 0$, $|G_{\mathrm{E}}| = |G_{\mathrm{M}}|$ and $|G_{\mathrm{E}}| = 3|G_{\mathrm{M}}|$. The first two are inspired by the data and the last one is connected with the theoretical estimates. Simulations have been done assuming high luminosity mode of HESR ($L = 2 \times 10^{32}$ cm^{-2}s^{-1} and $\sigma_{\mathrm{p}}/p \simeq 10^{-4}$) and running period of 4 months for each q^2 point, thus giving an integrated luminosity of 2 fb^{-1}.

The same analysis chain as for the background channels, i.e. with the same cuts on PID and CL, has been applied to the signal events. Fig. 5 shows the case $q^2 = 8.21$ (GeV/c)^2 value. Here one can see reconstructed angular distribution, as well as one after efficiency correction. One can clearly see, that after appling the efficiency correction (obtained from a distinct simulation using an isotopic distribution) we nicely reproduce the Monte Carlo distribution.

The integrated efficiency ($\cos\theta < |0.8|$) of PID cuts is decreasing with increasing q^2 (Fig. 6), from 40% for the low q^2 region down to 17% fat $q^2 = 22$ (GeV/c)^2. The efficiency of the kinematical constrainsts is almost constant over the full q^2 range.

The reconstruction efficiency depends strongly on $\cos\theta$: backward/forward angles are then strongly suppressed. Efficiency reaches very low values $|\cos\theta| > 0.8$ region. These inefficiencies at high $|\cos\theta|$ gets worse when going up in q^2.

The efficiency corrected angular distributions were fitted using a 2 parameter function. The ratio R of the form factors and the corresponding error bars have been extracted. Fig. 7 shows the expected errors on R for the $|G_{\mathrm{E}}| = |G_{\mathrm{M}}|$ case. Expectations for the measurement with the $\bar{\mathrm{P}}$ANDA detector are compared to the data points from the BaBar[8] and PS170[9] experiments. It is clear that the precision that can be achieved with $\bar{\mathrm{P}}$ANDA is an order of magnitude better then reached so far in other experiments. Moreover, $\bar{\mathrm{P}}$ANDA will measure at higher q^2 values where no data exist.

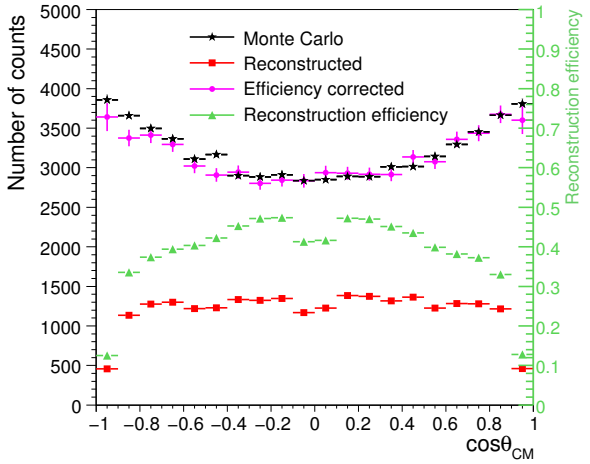

Fig. 5. The figure shows the angular distribution of e^+e^- pairs in the center os mass system. The black stars denote the distribution at the output of the event generator (Monte Carlo). The red squres denote the distribution of the reconstructed e^+e^- pairs. An acceptance and reconstruction efficiency correction (green triangle) has been determined from an isotropically in the CM distributed e^+e^- data sample (right scale). The angular distribution of the reconstructed and efficiency corrected e^+e^- pairs in the center os mass system at $q^2 = 8.21$ (GeV/c)^2 (pink dots).

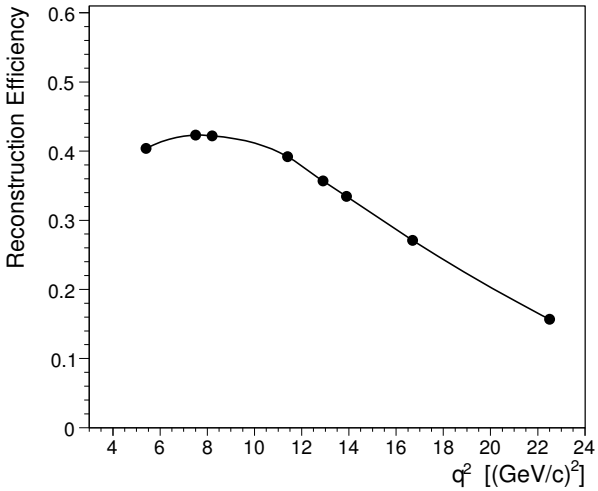

Fig. 6. Detection efficiency as a function of q^2. The averaged number for $|\cos\theta| < 0.8$ have been taken into account.

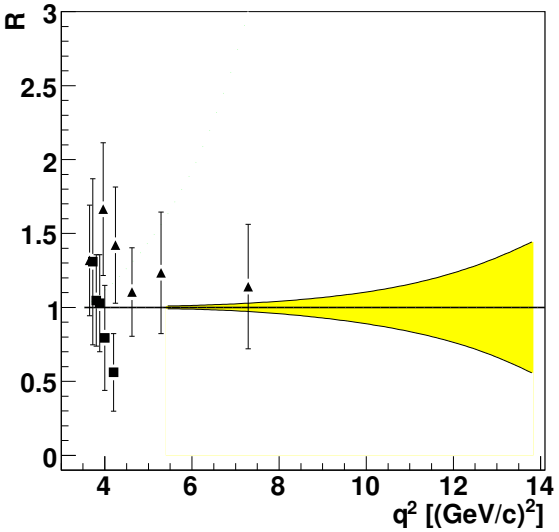

Fig. 7. The expected error of the ratio $R = |G_{\rm E}| = |G_{\rm M}|$ is given as a function of q^2. The yellow band represents the errors from the fits to the efficiency corrected e^+e^- distributions at 8 q^2 values.

4 Conclusion

The electromagnetic probe is an excellent tool to investigate the structure of the nucleon. The $\bar{\rm P}$ANDA experiment will offer the unique possibility for a precise determination of the electromagnetic form factors in the time-like region with unprecedented accuracy in a wide energy range. $\bar{\rm P}$ANDA will measure the ratio of the two proton form factors $G_{\rm E}$ and $G_{\rm M}$ with a precision ranging from <1% at low q^2 up to 30% for the $q^2 = 14$ (GeV/c)^2. While the analysis of the shape of the cross section gives access to the ratio, the precise luminosity monitor foreseen at $\bar{\rm P}$ANDA will allows the separate determination of $|G_{\rm E}|$ and $|G_{\rm M}|$. Above 14 (GeV/c)^2, the sensitivity for the extraction of R will become very poor, but it will still be possible to measure the cross section up to almost 27 (GeV/c)^2. This will allow us to enter a region where asymptotical behaviour might show up.

It is also interesting to investigate following reaction $\bar{\rm p}{\rm p} \to {\rm e}^+{\rm e}^-\pi^0$. This reaction could allow us to measure the form factors in the unphysical region, below the $\bar{\rm p}$p threshold ($q^2 = 4M_{\rm p}^2$). The energy range is analog to the so called Initial State Radiation employed on the e^+e^- collider experiments (BaBar for example). The pion is used to carry away energy and momentum, therefore making q^2 ranges of the virtual photon below threshold accessible.

Furthermore, a feasibility study of the use of a transversely polarized target is being evaluated. Such a target would give access to the relative phase of $G_{\rm E}$ and $G_{\rm M}$ in the time-like region. This would be the first measurement of the phase difference (the nucleon form factors are complex in the time-like region). The main issue in this domain is to gather as many results as possible in the time-like region and to compare them with space-like measurements. There are indeed predictions which establish clear relationship between the time-like complex form factors and the real space-like ones.

References

1 Tomasi-Gustafsson E, Rekalo M P. Phys. Lett. B, 2001, **504**: 291, and refs herein
2 Zichichi A et al. Nuovo Cimento, 1962, **XXIV**: 170
3 http://www-panda.gsi.de/auto/home.html
4 http://www.gsi.de/fair/overview/accelerator/index.html
5 http://www.gsi.de/fair/index.html
6 The PANDA Collaboration. arXiv:0903.3905
7 S. Ong et Van de Wiele: HAL : in2p3-00222925
8 Aubert B et al. Phys. Rev. D, 2006, **73**: 012005
9 Bardin G et al. Nucl. Phys. B, 1994, **411**: 3